Article details

Henneman B., Heinsman J., Battjes J. & Dame R.T. (2018), Quantitation of DNA-binding affinity using Tethered Particle Motion. In: Dame R.T. (Ed.) Bacterial Chromatin: Methods and Protocols. Methods in Molecular Biology no. 1837 New York, NY, U.S.A.: Humana Press. 257-275.
Doi: 10.1007/978-1-4939-8675-0_14

Chapter 14

Quantitation of DNA-Binding Affinity Using Tethered Particle Motion

Bram Henneman, Joost Heinsman, Julius Battjes, and Remus T. Dame

Abstract

The binding constant is an important characteristic of a DNA-binding protein. A large number of methods exist to measure the binding constant, but many of those methods have intrinsic flaws that influence the outcome of the characterization. Tethered Particle Motion (TPM) is a simple, cheap, and high-throughput single-molecule method that can be used to reliably measure binding constants of proteins binding to DNA, provided that they distort DNA. In TPM, the motion of a bead tethered to a surface by DNA is tracked using light microscopy. A protein binding to the DNA will alter bead motion. This makes it possible to measure binding properties. We use the bacterial protein Integration Host Factor (IHF) as an example to show how specific binding to DNA can be measured. Moreover, we show a new intuitive quantitative approach to displaying data obtained via TPM.

Key words Single molecule, Tethered particle motion, Root mean square, Displacement, DNA binding, Nucleoid associated protein, IHF

1 Introduction

Determination of binding affinity is an important part of the characterization of DNA-binding proteins. Typically, the binding affinity is expressed in terms of the binding constant (K_D). The K_D is the ratio of the off-rate constant, k_{off}, and the on-rate constant, k_{on}. Operationally, the K_D is defined as the concentration at which half of the substrate is bound by ligand (here: DNA and protein, respectively). For protein-DNA binding, the K_D is conventionally determined using Electrophoretic Mobility Shift Assays (EMSA), Filter Binding Assays, and Fluorescence Anisotropy [1–3]. Additionally, Isothermal Titration Calorimetry (ITC), Surface Plasmon Resonance (SPR) and Microscale Thermophoresis (MST) are used [4–6]. These techniques measure protein-DNA affinity in bulk, and therefore cannot distinguish different populations of bound and unbound molecules. Some of these techniques separate the protein-DNA complexes from solution or use small sample
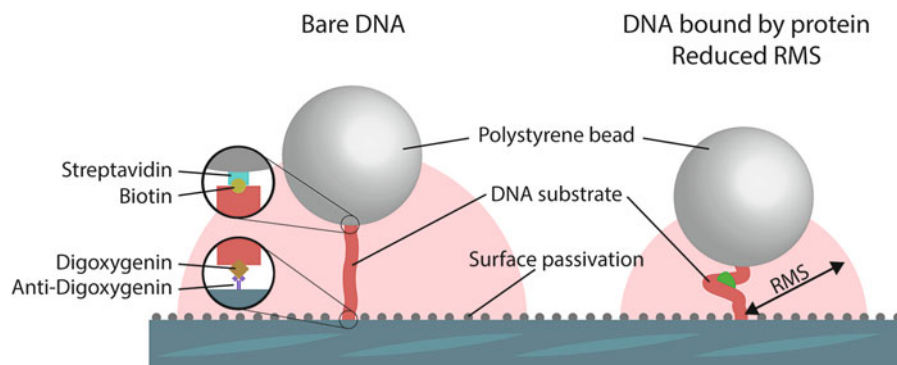
Fig. 1 Principle of Tethered Particle Motion (TPM). A bead is tethered to a glass surface by DNA. The position of the bead is tracked over time. Proteins that bind to the DNA and thereby deform it, change its apparent persistence length, which results in a change in the Root Mean Square displacement (RMS) of the bead

volumes, thus introducing large surface areas that may influence effective compound concentrations. Single-molecule techniques such as Optical Tweezers, Magnetic Tweezers, Acoustic Force Spectroscopy (AFS), and Atomic Force Spectrometry (AFM) can be used to estimate the K_D [7, 8], but require a high level of expertise and often expensive experimental setups. Single-molecule Förster Resonance Energy Transfer (smFRET) allows for measuring of DNA that is not bound to a surface and/or a bead [9], but requires fluorescently labeled DNA and protein and/or a sufficiently large and predictable conformational change of the DNA.

Tethered particle motion (TPM) is a simple, label-free single-molecule technique that can be used to characterize DNA-binding proteins in a high-throughput manner. The technique relies on the tracking of a bead in solution that has been tethered to a glass surface by a DNA molecule or other macromolecule (Fig. 1 and Fig. 2) [10]. The bead exhibits Brownian motion, which is restricted by the tether. In contrast to some of the above-mentioned techniques, no additional external force is applied to the bead. The xy-positions of the bead are recorded over time and are used to calculate the root mean square displacement (RMS) of the bead (Eq. 1). TPM has a high throughput (*see* **Note 1**), which makes it a powerful tool to study the characteristics of DNA-binding proteins. DNA-binding proteins that deform the DNA upon binding, change the apparent persistence length (L_p) of the DNA, a measure for rigidity, when bound, thereby altering the RMS [11]. Although the L_p cannot be directly calculated with TPM, the change in RMS is a reliable measure for protein binding. TPM has been used to measure DNA-binding by architectural proteins, proteins involved in DNA replication, transcription, DNA repair, and recombination [12–21].
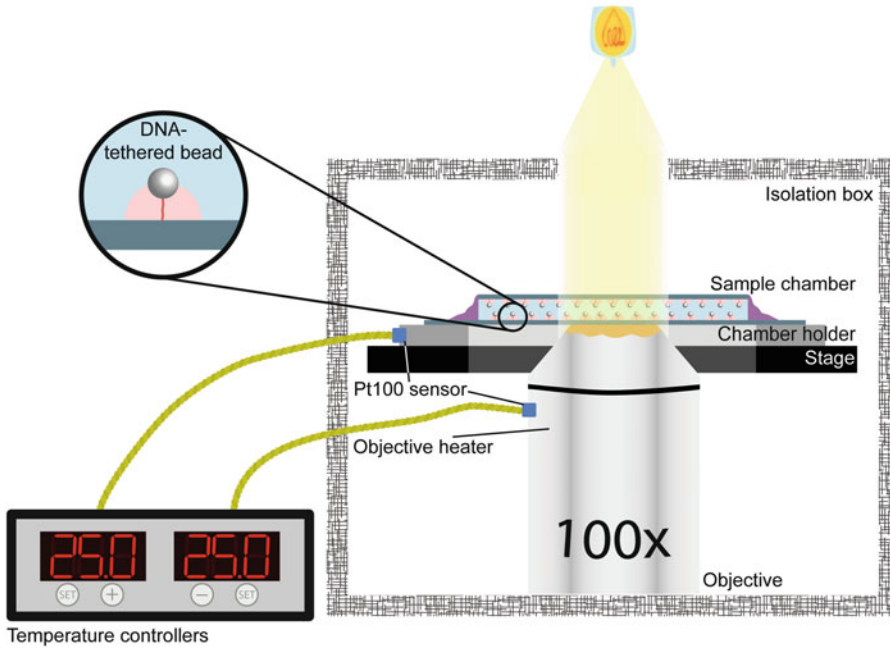
Fig. 2 Schematic of the Tethered Particle Motion setup. The sample chamber is heated by two heating elements, one placed in the sample chamber holder and one around the objective. An isolation box covers the stage, sample chamber and heating elements

$$\mathrm{RMS} = \sqrt{\frac{1}{n} \sum_{i=1}^{n} \left[(x_i - \bar{x})^2 + (y_i - \bar{y})^2 \right]} \qquad (1)$$

Equation 1 Calculation of the Root Mean Square displacement. x and y are the coordinates of the two-dimensional position of the bead.

In this chapter we describe the use of TPM to measure the K_D of sequence-specific DNA-binding proteins. As an example we characterized the bacterial Integration Host Factor (IHF) [22] from *E. coli*. IHF is a nucleoid-associated protein (NAP) that is involved in shaping genome architecture in bacteria. IHF also plays a role in up- and downregulation of genes [23]. This function is attributed to the ability of IHF to bend DNA and bring regulatory elements together, as well as due to direct interactions with RNA polymerase [24, 25]. IHF is known to bend DNA when bound at its high affinity recognition sequence [26] and also bends DNA when bound to DNA nonspecifically [27]. Bound at its specific site, binding angles of 120–160° have been reported [28–30].

2   Materials

2.1   Parafilm
Semi-Circles

1. Parafilm.
2. Office tape.
3. Laser cutter.
4. Computer-aided design (CAD) software (for example Auto-CAD or CorelDRAW).
5. Tweezers.

2.2   Sample
Chambers

1. Round cover glass, diameter 35 mm (VWR).
2. Round cover glass, diameter 28 mm (Thermo Scientific).
3. Parafilm semi-circles (see above).
4. Cover slip rack (Diversified Biotech).
5. Ethanol.
6. Acetone.
7. Beaker.
8. Sonication bath.
9. Heating block, capable of heating up to 100 °C, with hot plate for 35 mm cover glasses (*see* **Note 2**).
10. Tweezers with pointed tips.
11. KIMTECH SCIENCE* precision wipes tissue wipers (Kimberly-Clark).
12. Nitrile gloves (*see* **Note 3**).
13. Whatman paper.

2.3   Bead Suspension

1. Streptavidin-coated polystyrene beads, diameter 0.44 μm (Kisker Biotech).
2. Immersion sonicator with fine tip.
3. Bead buffer (BB) (10 mM Tris–HCl pH 7.5, 150 mM NaCl, 1 mM EDTA pH 8.0, 1 mM DTT, 3% glycerol, 100 μg/mL BSA-acetylated [Ambion]).
4. Vortex.

2.4   Anti-Digoxigenin
Solution

1. Anti-digoxigenin (anti-Dig) polyclonal antibodies 200 μg (Roche).
2. Bead buffer (BB) (see above).

2.5   DNA Substrate

1. Template for DNA substrate containing the binding site of interest. PCR amplification with compatible primers should yield a substrate of desired length and sequence (*see* **Note 4**).

2. Biotinylated forward primer, 10 μM in 10 mM Tris, pH 7.5, designed to be compatible with the template (*see* **Note 5**).

3. Digoxygenin-labeled reverse primer, 10 μM in 10 mM Tris, pH 7.5, compatible with the template (*see* **Note 5**).

4. Phusion master mix (New England Biolabs).

5. DMSO.

6. Milli-Q.

7. GenElute PCR clean-up kit (Sigma Aldrich).

8. PCR reaction tubes.

9. Biorad C1000 Thermal Cycler.

2.6 Substrate Quality Control

1. Agarose gel, 1% in Tris/Borate/EDTA (TBE) buffer.

2. GelRed nucleic acid gel stain (Biotium).

3. GeneRuler DNA marker.

4. Spectrophotometer to measure DNA concentrations (Nanodrop, Qubit, SimpliNano or comparable device).

2.7 Sample Chamber Reagents

1. Bead buffer (BB) (see above).

2. Anti-digoxigenin solution.

3. Passivation solution (4 mg/mL Blotting Grade Blocker [Bio-Rad] dissolved in SB).

4. Experimental buffer (EB) suitable for protein binding (*see* **Note 6**).

5. Protein of interest, preferably at high concentrations to avoid as much as possible components of the protein storage buffer on the EB (*see* **Note 7**).

2.8 Imaging

1. Isolation table.

2. Inverted microscope (Nikon Diaphot 300).

3. 100× oil-immersion objective (NA 1.25).

4. Immersion oil for microscopy (Merck).

5. Heat chamber (Bioscience tools TC-HLS-025 heating element for heating of the objective and a custom sample chamber heating element consisting of 40 parallel resistors); Pt100 sensors attached to the sample chamber holder and the objective, and two SA200 PID digital temperature controllers).

6. Climatized room.

7. Isolation box.

8. Thorlabs CMOS camera DCC1545M.

9. Lens paper.

10. Nacre-free nail polish.

11. Particle-tracking software (software available online [31]; *see* **Note 8**).

2.9 Data Analysis and Representation

1. Computer.

2. Custom MatLab routine for calculating RMS, standard deviation of the RMS and anisotropic ratio. The routine also selects the beads that meet the requirements for reliable beads (*see* Subheading 3.9).

3. Graphing and data analysis software, such as KaleidaGraph, Origin or IGOR Pro.

4. Adobe Illustrator.

3   Methods
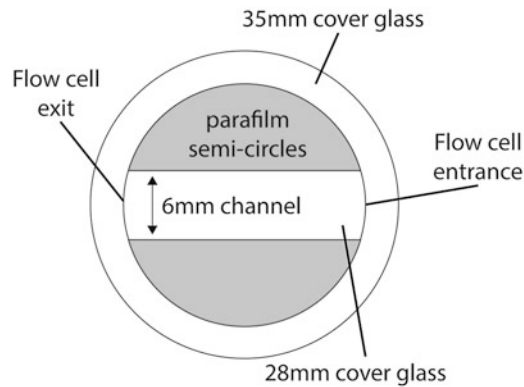
3.1 Parafilm Semi-Circles

1. Cut a strip of parafilm at a length fitting the grid of the laser cutter.

2. Remove the protection layer from the parafilm and place the parafilm onto the grid of the laser cutter.

3. Load the template of the semi-circles in the laser cutter software of choice. Design has to be such that two parafilm semi-circles on a 28 mm coverglass create a 6 mm wide channel. Position the parafilm so that the template virtually overlays the parafilm.

4. Fix the parafilm on the grid with office tape.

5. Cut the parafilm (*see* **Note 9**).

6. Remove parafilm strip. The semi-circles will stick to the grid of the laser cutter. Take the semi-circles off the grid individually with tweezers.

7. Store the parafilm semi-circles at 4 °C to prevent sticking to each other.

3.2 Sample Chambers

The following steps should be carried out with gloves, both to protect the hands from exposure to chemicals and to keep the sample chambers free of contaminants.

1. Place the cover glasses in the slide holder using the tweezers with pointed tips (*see* **Note 10**).

2. Place the holder in a beaker and submerge in acetone. Place the beaker in a sonication bath and sonicate for one cleaning cycle (*see* **Note 11**).

3. Transfer the slide holder into a new beaker and submerge the slide holder in ethanol. Place the beaker in a sonication bath and sonicate for one cleaning cycle.

4. Remove the holder from the beaker. Place the cover glasses on a precision wipe and dry the cover glasses by gently wiping them with precision wipes. Turn the cover glasses over and leave exposed to air for 10 min to dry.

Fig. 3 Sample chamber for TPM. The sample chamber consists of two parafilm semi-circles sandwiched between two cover glasses. The sample chamber is agglutinated by heating to 100 °C

5. Using tweezers place two parafilm semi-circles in parallel on opposing sides of a 28 mm cover glass, so that a straight channel is created (Fig. 3). The parafilm should align with the glass on the round edges. Push the parafilm firmly but carefully onto the cover glass with the tweezers so that the parafilm adheres to the cover glass (*see* **Note 12**).

6. Place the 35 mm cover glass on top of the parafilm-covered side of the 28 mm cover glass using tweezers, carefully centered onto the 28 mm cover glass. Push firmly but carefully with the tweezers so that the slides stick together.

7. Place the sample chamber on the hot plate (preheated to 100 °C) using tweezers. Cover the sample chamber with the lid and press firmly and evenly on the lid for 10 s. Remove the lid from the sample chamber (*see* **Note 13**).

8. Lift the sample chamber off the hot plate using tweezers and let it cool down on a precision wipe. Store the sample chamber in a small plastic storage box at room temperature.

3.3 **Bead Suspension**

1. Dilute the stock of streptavidin-coated beads to 0.01% w/v in 5 mL SB (*see* **Note 16**).

2. Vortex thoroughly for 5 min.

3. Sonicate the bead suspension on ice for 3 min (active), 2.5 s on and 9.9 s off, at 25% of the maximum power of the immersion sonicator. The total run time will be around 15 min. The tip of the immersion sonicator should be submerged by roughly 3 cm. Never sonicate the bead suspension for more than 5 min of active time, as this may damage the beads and its coating.

4. Flow 30 μL of bead suspension into an empty sample chamber. If less than 1% of the beads is clustered, it is considered a good bead suspension.

5. Store the bead suspension at 4 °C.

3.4 DNA Substrate

1. Add the following components to a PCR reaction tube on ice:

Component	Quantity
DNA template in 10 mM Tris pH 7.5	10 ng
Biotinylated forward primer	25 pmol
Digoxygenin-labeled reverse primer	25 pmol
Phusion master mix	25 μL
DMSO	1.5 μL
Milli-Q	To total volume of 50 μL

2. Place the PCR reaction tube in the thermal cycler and use the following touchdown protocol (*see* **Note 14**):

Temperature	Duration	Cycles
98 °C	30 s	
98 °C 72 °C (−1 °C per cycle) 72 °C	10 s 20 s 60 s	15×
98 °C 57 °C 72 °C	10 s 20 s 60 s	25×
72 °C	600 s	
12 °C	∞	

3. Purify the PCR product using a PCR clean-up kit (*see* **Note 15**).

4. Run 2 μL of PCR product on a 1% agarose gel, prestained with GelRed, alongside a suitable DNA marker. Verify the length of the DNA substrate and estimate the concentration using a spectrophotometer. Store the DNA substrate at −20 °C at a concentration of 100–500 pM.

3.5 Anti-Digoxygenin Solution

1. Dissolve 200 μg of anti-digoxygenin in 1 mL of BB.

2. Aliquot per 20 μL and store the anti-digoxygenin at −20 °C.

3. When using the anti-digoxygenin solution, thaw an aliquot and dilute 10 times with BB.

3.6 DNA-Tethered Bead in Sample Chamber

1. Take a clean sample chamber and flow in 20 µg/mL anti-dig solution by holding the tip of a pipette against the opening on the right side of the sample chamber at a 45° angle and carefully pressing the plunger button (*see* **Note 17**). Incubate for 10 min at room temperature.

2. Wash the sample chamber with 100 µL passivation solution and incubate for 10 min at room temperature. The excess liquid flowing out of the sample chamber is collected using Whatman paper. This promotes an undisturbed and uninterrupted flow in the channel.

3. Wash the sample chamber with 100 µL BB (*see* **Note 18**).

4. Flow in 100 µL 100 pM DNA substrate (*see* **Note 19**). Incubate for 10 min at room temperature.

5. Wash the sample chamber with 100 µL BB.

6. Pipette the bead suspension stock up and down and flow in 100 µL bead suspension. Incubate for 10 min at room temperature.

7. Wash the sample chamber with 100 µL EB.

8. Flow in 100 µL protein solution, diluted to the desired concentration in EB. Incubate for 10 min at room temperature.

9. Wash the sample chamber with 100 µL protein solution of the same concentration as in **step 8**.

10. Seal the sample chamber on both sides by applying nail polish to the opening of the sample chamber. When the nail polish is dry, the sample chamber is ready to be used.

3.7 Dilution Series

1. Calculate a dilution series with a range from 0 to 1000 nM using twofold dilution steps (*see* **Note 20**). Determine the concentration range in which DNA binding is to be expected. Literature values can be used if available; if not, preliminary experiments may be required.

2. Dilute a protein stock aliquot to a concentration that can be used to make further protein dilutions with EB (*see* **Note 21**). Store this stock on ice (*see* **Note 22**).

3. Using the working stock, make a dilution series by diluting part of the working stock with EB to the desired concentration. Dilute part of this sample with EB in order to create the next sample (*see* **Note 21**). Store samples on ice (*see* **Note 22**).

4. Measure at least two, but preferably three dilution series (*see* **Note 23**).

3.8 Imaging

1. An hour before imaging, turn on the lamp and the heating stage.

2. Place immersion oil on the objective and start imaging software.

3. Place a sample chamber in the sample chamber holder.

4. Raise the objective until the beads are in focus (*see* **Note 24**).

5. Close the isolation chamber. The temperature of the chamber and the objective will now rise to a set temperature (*see* **Note 25**).

6. Re-focus on the beads and ensure that no focal drift is observed (*see* **Note 26**).

7. Select a field of view by moving the stage of the microscope. Select the beads and track them for at least 1500 frames. Images are taken at 25 Hz, with an exposure time of 20 ms. At least 100 "good" bead-tether combinations are needed for quantification after quality check (explained in Subheading 3.9; *see* **Note 27**).

8. Use the tracking software to determine x- and y-positions of the beads (*see* **Note 8**).

3.9   Data Analysis

1. Calculate the anisotropic ratio (Eq. 2), the root mean square displacement (RMS) and the standard deviation of the RMS for all measurements at a given concentration combined (*see* **Note 28**). Discard tethers with an anisotropic ratio of above 1.3. Discard measurements with a standard deviation of the RMS larger than 6% of the RMS. We thereby exclude beads sticking to the surface during the measurement (*see* **Note 29**).

2. Plot all RMS values that meet the requirements as explained in **step 1** a in a histogram.

3. Fit a Gaussian curve to the histogram to determine the average RMS and standard deviation for each condition.

4. Calculate the standard error of the mean for each condition.

$$\alpha = \frac{l_{\mathrm{major}}}{l_{\mathrm{minor}}} \tag{2}$$

Equation 2 Calculation of the anisotropic ratio (α). l_{major} and l_{minor} represent the length of the major and minor axis of the xy-scatter plot, respectively.

3.10   Analysis of Specific Protein-DNA Binding

1. Determine the RMS of the DNA-tethered bead in the absence of protein. This is the position of the peak in the Gaussian fit at 0 nM (Fig. 4a).

2. Determine the RMS at saturation levels of specific binding. This is the concentration at which the peak seen at 0 nM has completely disappeared and a peak at a different RMS has appeared (Fig. 4f).

3. Concentrations at which two peaks are observed, represent a situation in which a subpopulation of the DNA is bound by protein (Fig. 4b–e).
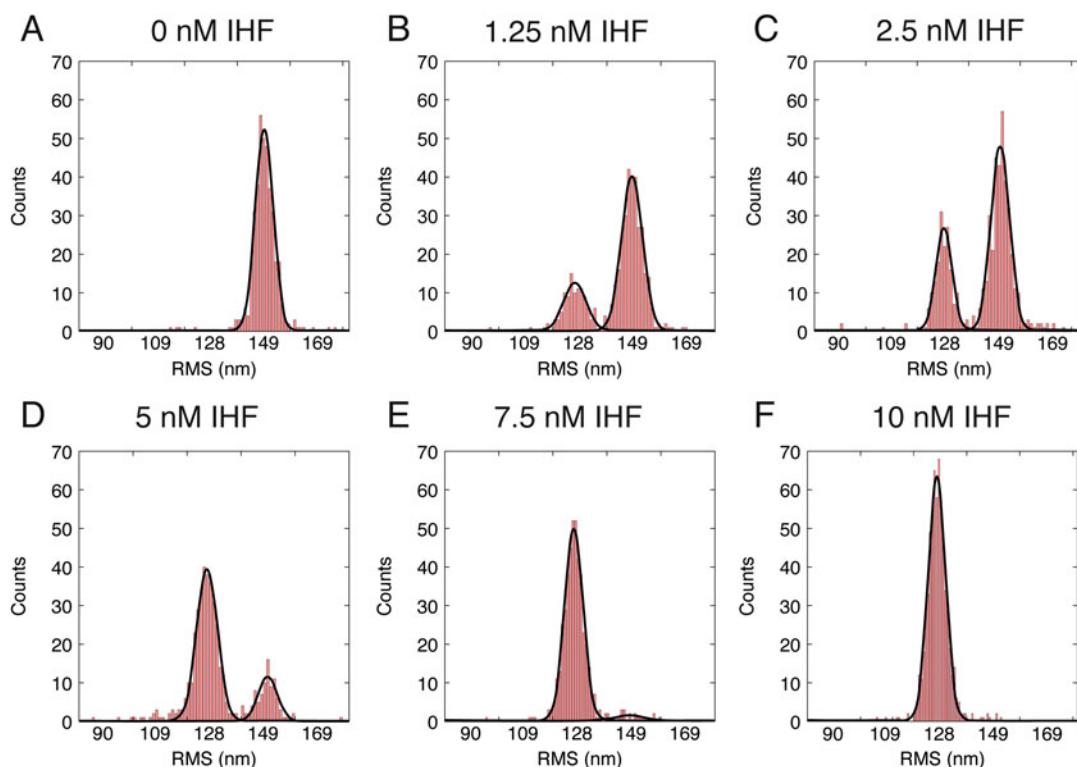
Fig. 4 Specific binding of IHF to DNA at 0–10 nM. (**a–f**) histograms of RMS values obtained for DNA-tethered beads at IHF concentrations of 0, 1.25, 2.5, 5, 7.5, and 10 nM. The histograms have been fitted with a Gaussian function in KaleidaGraph (black, semi-opaque line)

4. For the concentrations at which subpopulations of bound and unbound states can be observed, calculate the occupancy (Eq. 3). Occupancy is the ratio between bound and unbound DNA substrates.

5. Find the K_D and Hill coefficient (n) by solving the Hill binding model (Eq. 4) for K_D and n (*see* **Note 30**).

6. Fit the occupancies using the Hill-binding model (Fig. 5; *see* **Note 31**). Use graphing and data analysis software to display the occupancies per concentration and the Hill fit in a graph.

3.11 Example of K_D Estimation for DNA-Binding Protein IHF

We used IHF as an example to illustrate how to characterize specific DNA binding proteins. In our example, we observe a reduction in RMS at low (1.25 nM) IHF concentrations from 149 to 127 nm (Fig. 4). This reduction in RMS is caused by DNA bending as a consequence of IHF binding at its specific binding site (*see* **Note 32**). Saturation of specific binding is achieved at 10 nM, the concentration at which only the population with reduced RMS is observed. Fitting the data using the Hill binding model (χ^2: 4.6) yields a binding affinity (K_D) of 3.0 ± 0.3 nM, which is in
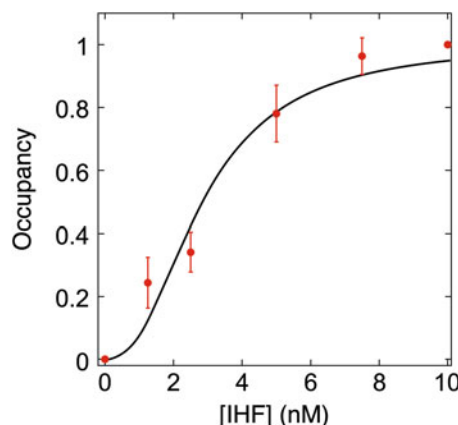
Fig. 5 Binding curve for specific binding of IHF to DNA. The data points were fit using the Hill-binding model. The Hill coefficient (*n*) is 2.5 ± 0.5, and the binding affinity (K_D) is 3.0 ± 0.3 nM. Error bars represent the standard error of the mean

agreement with values reported using EMSA on different variants of the binding consensus sequence [32]. A Hill coefficient (*n*) of 2.5 ± 0.5 was found. A Hill coefficient >1 indicates positively cooperative binding; $n < 1$ indicates negatively cooperative binding (*see* **Note 33**).

$$\theta = \frac{h_{\text{peak, bound}}}{h_{\text{peak, bound}} + h_{\text{peak, unbound}}} \tag{3}$$

Equation 3 Calculation of occupancy. The occupancy is the fraction of substrate bound by protein and can be calculated from the area of the peaks of the fitted Gaussian distributions.

$$\theta = \frac{1}{\left(\frac{K_D}{[L]}\right)^n + 1} \tag{4}$$

Equation 4 Hill binding model. Occupancy θ, binding constant K_D, ligand concentration $[L]$, Hill coefficient *n*.

3.12 Data Representation

TPM is a single molecule method with a high throughput. As a consequence data are often reported in terms of an average RMS value. However, displaying the full population of RMS values can be insightful to illustrate distribution shape and population heterogeneity. The new representation approach presented here accommodates both average values, as well as unprocessed population information.

1. Plot all data points as black squares using the graphing and analysis software.

2. In the same plot, include the values of the average RMS at all concentrations and display in a color different from that of the data points.
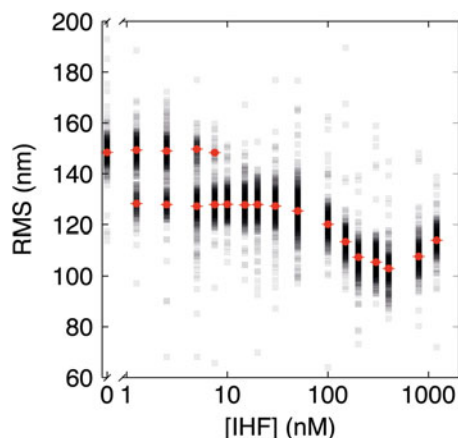
Fig. 6 Compaction of DNA by IHF. Black, partially transparent squares represent the individual RMS values of DNA-bead complexes after application of anisotropic ratio and standard deviation of the RMS as selection criteria. Red dots and bars represent the average RMS that resulted from fitting with a Gaussian function

3. Export the plot as a vector image.

4. Open the plot in Adobe Illustrator and select all black squares. Change the opacity from 100% to 5% (Fig. 6; *see* **Note 34**).

In our example, specific and nonspecific binding by IHF can be observed. Specific binding of IHF is observed between 0 and 10 nM, where the RMS decreases from 149 ± 5 nm to 127 ± 5 nm and is characterized by the two populations. Intensity profiles of the populations are equivalent to the histograms of Fig. 4. In the nonspecific binding regime, at IHF concentrations >30 nM, we find a single population of which the RMS continues to reduce as a function of IHF concentration up to 400 nM. This further reduction in RMS is reduced to sequence unspecific binding of the protein. At concentrations >400 nM the RMS increases, which is attributed to stiffening of DNA by IHF bound at high density along the DNA, similar to the effects of observed for the HU protein [33].

4   Notes

1. Up to 100 beads were measured for 1 min.

2. A custom-made hot plate was used to heat the sample chambers. The hot plate is made from a circular massive metal block in which a shallow cavity is carved (diameter 35 mm). A sample chamber fits into the cavity. A metal lid (diameter 35 mm) with a plastic handle covers the sample chamber. The hot plate is

placed on a heating block and heats the sample chamber to 100 °C.

3. Nitrile gloves were used, as the powder that is often found in rubber gloves may contaminate the sample chamber.

4. As a template the plasmid pGp1 was used [34], which contains part of the bacteriophage mu genome. A 685 bp fragment that contains 1 IHF-binding site exactly at the center was amplified, which is expected to result in the highest effect on end-to-end distance [30]. Our experience is that a DNA substrate in the order of 700 bp is ideal, as protein binding results in a clearly detectable change in RMS.

5. The forward and reverse primers that we used are 5' BIO-TGATTAAGGTTGTGGTTAATTTGTTATCAGTTCC-G3' and 5' DIG-ATTACTTCCGGTTTAGTTTCTAAGGCG 3', respectively.

6. The experimental buffer contained 10 mM Tris–HCl pH 8.0 and 100 mM KCl, which is suitable for specific binding of IHF [35]. The osmolarity of the buffer should be sufficiently high to prevent nonspecific binding of specific binding proteins. A different protein of interest may require buffer optimization.

7. Recombinant *E. coli* IHF at a concentration of 120 μM was used here. This stock was diluted 100-fold at minimum. The number of freeze-thaw cycles was minimized by aliquoting the protein stock, to guarantee protein activity.

8. Software written for Acoustic Force Spectrometry was used [31], which is freely available online (http://figshare.com/articles/AFS_software/1195874). Other particle tracing software has been described and compared by Chenouard et al. [36]. Our lab also has positive experience with Poly-ParticleTracker [37].

9. Here, the computer-aided design software AutoCAD was used to design the cutting template in combination with the Versa-Laser tabletop Laser cutter. We cut the parafilm at 55% laser power, 30% of the maximum speed, 1000 pulse and 1.00 mm Z-axis. Different laser cutters may require different settings, allowing the parafilm to be cut straight and without melting or burning.

10. Ensure that each slot is occupied by only one cover glass. The cover glasses tend to stick together, which prevents them from being cleaned properly.

11. For sonication of the glass slides, the Emag EMMI 4 sonicator was used, which is pre-programmed in cycles of 9 min at 42.5 kHz.

12. Note that the parafilm leaves grease marks on the cover glass, so avoid sliding after placing them.

13. Heating the sample chamber for too long may result in excessive melting of the parafilm, which causes a non-straight sample chamber. This prevents a good flow in the sample chamber. As a result, coating of the surface with anti-digoxygenin and/or passivation agent may be heterogenous, which reduces throughput and results in lower effective protein concentrations. Especially experiments at low concentration may then suffer from reduced reproducibility.

14. Conventional protocols with fixed annealing temperatures may be used as well, but need to be individually optimized for different primer-template combinations and synthesized fragment lengths.

15. Purification using the GenElute PCR clean-up kit separates the PCR product from other components that were added to the reaction tube to facilitate the PCR reaction, such as excess primers, nucleotides, and salts. The result of this purification is the labeled DNA substrate in 10 mM Tris–HCl pH 8.5 (provided with the kit).

16. The bead stock is vortexed and sonicated to homogenize the suspension. Beads tend to stick together, which will distort measurements.

17. Check if the sample chamber has no cracks in either of the cover glasses, as defects may create a flow inside the sample chamber while measuring. This will affect the RMS by giving it a directional bias. Also, check if the channel is straight; *see* Fig. 3. Left-handed people may prefer using the opening on the left side of the sample chamber for sample loading.

18. The volumes used for washing depend on the volume of the sample chamber. As a rule of thumb, we wash with approximately three times the volume of the sample chamber.

19. The DNA substrate concentration is 100 pM, but when we find that this concentration is not sufficient for a particular experiment, we raise the concentration up to 500 pM.

20. A dilution series with concentrations from 0 to 1000 nM is used, with twofold dilution steps. Based on results and literature values, an additional range and/or different dilution steps may be used, which may result in a more reliable calculation of the K_D.

21. When measuring many samples, consider breaking up the dilution series in two or more overlapping ranges. Here, we diluted a 120 μM IHF stock to a working stock of 1.2 μM. From that, we made a serial dilution which included IHF concentrations of 800, 400, 300, 200, 150, 100, and 50 nM: the high range concentrations. For the low range concentrations, we diluted the 1.2 μM working stock directly to 50 nM, from which we

subsequently made a serial dilution which included IHF concentrations of 30, 20, 15, 10, 7.5, 5, 2.5, and 1.25 nM. We verified that the RMS values at 50 nM from the high range dilution series were identical to the RMS values at 50 nM from the low range dilution series. We also measured the RMS in the absence of IHF, indicated with 0 nM.

22. Do not freeze the protein solutions, since the activity of the protein may be affected.

23. For reliable results and to minimize the effect of pipetting errors, experiments should be carried out at least in duplo, but preferably in triplo, and independently of each other. Especially when the concentration range over which binding takes place is narrow, small changes in sample concentrations can be of significant influence on the outcome of the binding curve.

24. Due to a sedimentation effect, there may be a slight difference in RMS between beads tethered to the bottom surface and beads tethered to the top surface. Therefore, always choose the same surface for measurements. Also, the focus for top and bottom surfaces may differ.

25. It may take 5–20 min, depending on the temperature, before the isolation chamber has completely reached the desired temperature.

26. While the temperature of the immersion oil on the objective rises, the refractive index of the oil changes slightly. As a result, focal drift is observed. Wait until the immersion oil has reached the desired temperature and then refocus. When no focal drift is observed, the immersion oil has the desired temperature.

27. At least 100 good bead-tether combinations are needed, but the actual amount of measured bead-tether combinations to reach this limit may differ. For IHF, 300 measured bead-tether combinations always resulted in more than 100 good combinations. The amount of bead-tether combinations that need to be measured, depends on the protein that is used.

28. Verify that individual experiments done at the same concentration give similar outcomes. If so, RMS values can be combined and can be fitted together. If one measurement is a clear outlier due to a known cause, discard the measurement. In other cases, re-measure the sample and check if the results align with any previous measurements.

29. Discard any bead with an anisotropic ratio >1.3, which is considered non-symmetrical. Non-symmetrical beads indicate for example that a bead is attached to two DNA tethers. An extensive study that links motion patterns to setup defects has been done by Visser et al. [38]. Also discard any bead with a standard deviation of the RMS of >6%, since this indicates

rapid protein dissociation and sticking and/or releasing of the bead to or from the sample chamber surface.

30. The Hill equation can be solved using IGOR Pro, which was done here, but MatLab and other data analysis programs are also suitable for this.

31. As error bars, the standard error of the mean of the individual measurement series per concentration has been used.

32. If desired, the effective persistence length of the DNA can be determined for a single protein bound to DNA, which could be used to calculate the DNA bending angle as described by Kulić and coworkers [11]. However, this requires an extensive simulation series, which reveals the relation between RMS and L_p. The simulations are highly dependent on the length and sequence of the DNA substrate, buffer conditions, and temperature of the experiment. This means that for every experiment in which one or more of these parameters are changed, a new simulation series is required. The simulations have been described by Driessen et al. [39].

33. Here, the Hill coefficient is 2.5, which indicates positively cooperative binding. However, in this example, only one IHF dimer binds to DNA. The apparent positively cooperative binding is possibly a result of the dimeric nature of the protein. Both components of the dimer have to bind to the DNA in order to bend the DNA.

34. For representation of all data points, squares are most suitable, because squares are easy distinguishable when data points overlap. Circles may make it harder to distinguish individual data points in the plot. The opacity that suits your data best depends on the number of data points. When using more data points than shown in the example, it may be useful to use a lower opacity. The Gaussian distribution of the data points should be visible from the intensity of the combination of data points.

Acknowledgments

References

1. Hellman LM, Fried MG (2007) Electrophoretic mobility shift assay (EMSA) for detecting protein-nucleic acid interactions. Nat Protoc 2 (8):1849–1861. https://doi.org/10.1038/nprot.2007.249

2. Gilman AG (1970) A protein binding assay for adenosine 3′:5′-cyclic monophosphate. Proc Natl Acad Sci U S A 67(1):305–312

3. Heyduk T, Ma Y, Tang H, Ebright RH (1996) Fluorescence anisotropy: rapid, quantitative

assay for protein-DNA and protein-protein interaction. Methods Enzymol 274:492–503

4. Ziegler A, Seelig J (2007) High affinity of the cell-penetrating peptide HIV-1 tat-PTD for DNA. Biochemistry 46(27):8138–8145. https://doi.org/10.1021/bi700416h

5. Hart DJ, Speight RE, Cooper MA, Sutherland JD, Blackburn JM (1999) The salt dependence of DNA recognition by NF-kappaB p50: a detailed kinetic analysis of the effects on affinityand specificity. Nucleic Acids Res 27 (4):1063–1069

6. Jerabek-Willemsen M, Wienken CJ, Braun D, Baaske P, Duhr S (2011) Molecular interaction studies using microscale thermophoresis. Assay Drug Dev Technol 9(4):342–353. https://doi.org/10.1089/adt.2011.0380

7. Yang Y, Sass LE, Du C, Hsieh P, Erie DA (2005) Determination of protein-DNA binding constants and specificities from statistical analyses of single molecules: MutS-DNA interactions. Nucleic Acids Res 33(13):4322–4334. https://doi.org/10.1093/nar/gki708

8. McCauley MJ, Williams MC (2011) Measuring DNA-protein binding affinity on a single molecule using optical tweezers. Methods Mol Biol 749:305–315. https://doi.org/10.1007/978-1-61779-142-0_21

9. Coats JE, Lin Y, Rueter E, Maher LJ 3rd, Rasnik I (2013) Single-molecule FRET analysis of DNA binding and bending by yeast HMGB protein Nhp6A. Nucleic Acids Res 41 (2):1372–1381. https://doi.org/10.1093/nar/gks1208

10. Schafer DA, Gelles J, Sheetz MP, Landick R (1991) Transcription by single molecules of RNA polymerase observed by light microscopy. Nature 352(6334):444–448. https://doi.org/10.1038/352444a0

11. Kulic IM, Mohrbach H, Thaokar R, Schiessel H (2007) Equation of state of looped DNA. Phys Rev E Stat Nonlinear Soft Matter Phys 75 (1 Pt 1):011913. https://doi.org/10.1103/PhysRevE.75.011913

12. van der Valk RA, Vreede J, Qin L, Moolenaar GF, Hofmann A, Goosen N, Dame RT (2017) Mechanism of environmentally driven conformational changes that modulate H-NS DNA-bridging activity. elife 6:e27369. https://doi.org/10.7554/eLife.27369

13. Driessen RP, Lin SN, Waterreus WJ, van der Meulen AL, van der Valk RA, Laurens N, Moolenaar GF, Pannu NS, Wuite GJ, Goosen N, Dame RT (2016) Diverse architectural properties of Sso10a proteins: evidence for a role in chromatin compaction and organization. Sci Rep 6:29422. https://doi.org/10.1038/srep29422

14. Chintakayala K, Sellars LE, Singh SS, Shahapure R, Westerlaken I, Meyer AS, Dame RT, Grainger DC (2015) DNA recognition by Escherichia coli CbpA protein requires a conserved arginine-minor-groove interaction. Nucleic Acids Res 43(4):2282–2292. https://doi.org/10.1093/nar/gkv012

15. Wang H, Yehoshua S, Ali SS, Navarre WW, Milstein JN (2014) A biomechanical mechanism for initiating DNA packaging. Nucleic Acids Res 42(19):11921–11927. https://doi.org/10.1093/nar/gku896

16. Mack AH, Schlingman DJ, Salinas RD, Regan L, Mochrie SG (2015) Condensation transition and forced unravelling of DNA-histone H1 toroids: a multi-state free energy landscape. J Phys Condens Matter 27 (6):064106. https://doi.org/10.1088/0953-8984/27/6/064106

17. Wu HY, Lu CH, Li HW (2017) RecA-SSB interaction modulates RecA nucleoprotein filament formation on SSB-wrapped DNA. Sci Rep 7(1):11876. https://doi.org/10.1038/s41598-017-12213-w

18. Lu CH, Li HW (2017) DNA with different local torsional states affects RecA-mediated recombination progression. ChemPhysChem 18(6):584–590. https://doi.org/10.1002/cphc.201601281

19. Fan HF, Cheng YS, Ma CH, Jayaram M (2015) Single molecule TPM analysis of the catalytic pentad mutants of Cre and Flp site-specific recombinases: contributions of the pentad residues to the pre-chemical steps of recombination. Nucleic Acids Res 43(6):3237–3255. https://doi.org/10.1093/nar/gkv114

20. Fan HF, Hsieh TS, Ma CH, Jayaram M (2016) Single-molecule analysis of varphiC31 integrase-mediated site-specific recombination by tethered particle motion. Nucleic Acids Res 44(22):10804–10823. https://doi.org/10.1093/nar/gkw861

21. Chen YF, Lu CY, Lin YC, Yu TY, Chang CP, Li JR, Li HW, Lin JJ (2016) Modulation of yeast telomerase activity by Cdc13 and Est1 in vitro. Sci Rep 6:34104. https://doi.org/10.1038/srep34104

22. Mangan MW, Lucchini S, Danino V, Croinin TO, Hinton JC, Dorman CJ (2006) The integration host factor (IHF) integrates stationary-phase and virulence gene expression in Salmonella enterica serovar Typhimurium. Mol Microbiol 59(6):1831–1847. https://doi.org/10.1111/j.1365-2958.2006.05062.x

23. Peacock S, Weissbach H, Nash HA (1984) In vitro regulation of phage lambda cII gene expression by Escherichia coli integration host factor. Proc Natl Acad Sci U S A 81 (19):6009–6013

24. Goosen N, van de Putte P (1995) The regulation of transcription initiation by integration host factor. Mol Microbiol 16(1):1–7

25. Khodr A, Fairweather V, Bouffartigues E, Rimsky S (2015) IHF is a trans-acting factor implicated in the regulation of the proU P2 promoter. FEMS Microbiol Lett 362(3):1–6. https://doi.org/10.1093/femsle/fnu049

26. Wang S, Cosstick R, Gardner JF, Gumport RI (1995) The specific binding of Escherichia coli integration host factor involves both major and minor grooves of DNA. Biochemistry 34 (40):13082–13090

27. Swinger KK, Rice PA (2004) IHF and HU: flexible architects of bent DNA. Curr Opin Struct Biol 14(1):28–35. https://doi.org/10.1016/j.sbi.2003.12.003

28. Rice PA, Yang S, Mizuuchi K, Nash HA (1996) Crystal structure of an IHF-DNA complex: a protein-induced DNA U-turn. Cell 87 (7):1295–1306

29. Travers A (1997) DNA-protein interactions: IHF--the master bender. Curr Biol 7(4): R252–R254

30. Dame RT, van Mameren J, Luijsterburg MS, Mysiak ME, Janicijevic A, Pazdzior G, van der Vliet PC, Wyman C, Wuite GJ (2005) Analysis of scanning force microscopy images of protein-induced DNA bending using simulations. Nucleic Acids Res 33(7):e68. https://doi.org/10.1093/nar/gni073

31. Sitters G, Kamsma D, Thalhammer G, Ritsch-Marte M, Peterman EJ, Wuite GJ (2015) Acoustic force spectroscopy. Nat Methods 12 (1):47–50. https://doi.org/10.1038/nmeth.3183

32. Yang SW, Nash HA (1995) Comparison of protein binding to DNA in vivo and in vitro: defining an effective intracellular target. EMBO J 14(24):6292–6300

33. van Noort J, Verbrugge S, Goosen N, Dekker C, Dame RT (2004) Dual architectural roles of HU: formation of flexible hinges and rigid filaments. Proc Natl Acad Sci U S A 101 (18):6969–6974. https://doi.org/10.1073/pnas.0308230101

34. Giphart-Gassler M, Goosen T, van Meeteren A, Wijffelman C, van de Putte P (1979) Properties of the recombinant plasmid pGP1 containing part of the early region of bacteriophage mu. Cold Spring Harb Symp Quant Biol 43(Pt 2):1179–1185

35. Holbrook JA, Tsodikov OV, Saecker RM, Record MT Jr (2001) Specific and non-specific interactions of integration host factor with DNA: thermodynamic evidence for disruption of multiple IHF surface salt-bridges coupled to DNA binding. J Mol Biol 310(2):379–401. https://doi.org/10.1006/jmbi.2001.4768

36. Chenouard N, Smal I, de Chaumont F, Maska M, Sbalzarini IF, Gong Y, Cardinale J, Carthel C, Coraluppi S, Winter M, Cohen AR, Godinez WJ, Rohr K, Kalaidzidis Y, Liang L, Duncan J, Shen H, Xu Y, Magnusson KE, Jalden J, Blau HM, Paul-Gilloteaux P, Roudot P, Kervrann C, Waharte F, Tinevez JY, Shorte SL, Willemse J, Celler K, van Wezel GP, Dan HW, Tsai YS, Ortiz de Solorzano C, Olivo-Marin JC, Meijering E (2014) Objective comparison of particle tracking methods. Nat Methods 11(3):281–289. https://doi.org/10.1038/nmeth.2808

37. Rogers SS, Waigh TA, Zhao X, Lu JR (2007) Precise particle tracking against a complicated background: polynomial fitting with Gaussian weight. Phys Biol 4(3):220–227. https://doi.org/10.1088/1478-3975/4/3/008

38. Visser EW, van IJ, Prins MW (2016) Particle motion analysis reveals nanoscale bond characteristics and enhances dynamic range for biosensing. ACS Nano 10(3):3093–3101. https://doi.org/10.1021/acsnano.5b07021

39. Driessen RP, Sitters G, Laurens N, Moolenaar GF, Wuite GJ, Goosen N, Dame RT (2014) Effect of temperature on the intrinsic flexibility of DNA and its interaction with architectural proteins. Biochemistry 53(41):6430–6438. https://doi.org/10.1021/bi500344j